Drug Delivery and Translational Research
https://doi.org/10.1007/s13346-025-01951-4

ORIGINAL ARTICLE

Critical evaluation of saponin as a permeabilizer for anandamide encapsulation in extracellular vesicles

Marie Auquière[1,2] · Romano Terrasi[2] · Viridiane Gratpain[1,5] · Jessica Vanderstraeten[1] · André Cronemberger-Andrade[4] · Negar Mozaheb[3,6] · Marie-Paule Mingeot-Leclercq[3] · Anne des Rieux[1] · Giulio G. Muccioli[2]

Accepted: 3 August 2025

Abstract

Extracellular Vesicles (EV) have received considerable attention as drug delivery systems. Research into the loading of various exogenous cargoes in EV has been expanding in recent years. While bioactive lipids are a class of highly interesting molecules, their loading in EV remains much less explored. Here, EV isolated from a microglial cell line were loaded with the endocannabinoid anandamide (AEA), using different approaches: passive incubation, sonication and permeabilization by saponin. The addition of saponin increased the amount of AEA detected in the EV suspension, as compared to passive incubation or sonication. However, our subsequent observations demonstrated that the higher quantity of AEA measured when using saponin was due to AEA solubilization into saponin micelles. The elimination of residual saponin differs according to the purification method used. Here, ultrafiltration (UF) did not eliminate saponin micelles, leading to a co-isolation of AEA-loaded EV and AEA-loaded micelles. In addition to AEA quantification by UPLC-MS/MS, we applied the generalized polarization (GP) value of Laurdan to study the impact of AEA incubation on the EV membrane. Our data show that AEA increased EV membrane fluidity, supporting AEA insertion into the membrane of the EV. More generally, this work raises awareness about the use of saponin as a permeabilizer for bioactive lipids encapsulation in EV.

Keywords Endocannabinoid · Micelles · Bioactive lipid · AEA · Laurdan · SEC · Ultrafiltration

Introduction

Extracellular vesicles (EV), including exosomes, are biological nanoparticles secreted by most cell types. EV have gained considerable scientific interest due to their potential for diverse biomedical applications, including diagnostic biomarkers, therapeutics or drug delivery systems [1]. Their low immunogenicity, biocompatibility, and ability to cross biological barriers make them particularly attractive for nanomedicine development [2]. Moreover, the loading of therapeutic molecules into EV has been shown to enhance

Anne des Rieux and Giulio G. Muccioli contributed equally to this work.

✉ Anne des Rieux
anne.desrieux@uclouvain.be

✉ Giulio G. Muccioli
giulio.muccioli@uclouvain.be

[1] Louvain Drug Research Institute, Advanced Drug Delivery and Biomaterials (ADDB), Université Catholique de Louvain, UCLouvain, Brussels 1200, Belgium

[2] Louvain Drug Research Institute, Bioanalysis and Pharmacology of Bioactive Lipids (BPBL), Université Catholique de Louvain, UCLouvain, Brussels 1200, Belgium

[3] Louvain Drug Research Institute, Cellular & Molecular Pharmacology Unit (FACM), Université Catholique de Louvain, Brussels, UCLouvain, Brussels 1200, Belgium

[4] Nanomédecine, Biologie Extracellulaire, Intégratome et Innovations en santé (NABI), Université Paris Cité, CNRS UMR8175, INSERM U1334, 45 rue des Saints Pères, Paris 75006, France

[5] Present address: Ipsen Manufacturing & R&D, Dreux 28 100, France

[6] Present address: Johnson & Johnson Innovative Medicine, Brussels, Belgium

Published online: 21 August 2025

drug stability, bioavailability, and delivery to specific target cells or tissues [3].

Several strategies have been explored to load drugs into EV. The most straightforward method involves co-incubating the drug with EV. However, the efficiency of this passive method strongly depends on the ability of the molecules to interact with or cross the EV membranes and can be limited [4]. To overcome low loading efficiency, active loading methods have thus been used as an alternative. These involve a transient disruption of the EV membrane to facilitate the incorporation of molecules either into the EV lumen or within its lipid bilayer. Physical techniques like sonication, extrusion or electroporation, as well as chemical techniques using surfactants, have been used to load various molecules in EV [2, 5]. The most well-known biosurfactant for this purpose is saponin, an amphiphilic glycoside composed of sapogenin and one or more oligosaccharide moieties. Saponin permeabilizes the lipid membrane by forming pores in the EV membrane [5, 6]. While other synthetic surfactants such as Triton X-100, Tween 80, or Lipofectamine can theoretically enhance membrane permeability, they are frequently associated with substantial disruption of membrane integrity and reduced biocompatibility. In contrast, saponin appears to provide a more favorable profile, enabling transient membrane permeabilization while preserving EV morphology and surface marker expression [7].

While various active loading strategies have been developed, most efforts have concentrated on hydrophilic molecules such as nucleic acids, proteins/peptides, and chemotherapeutic agents, and very few have explored the loading of bioactive lipids [8]. Bioactive lipids such as endocannabinoids are key signaling mediators involved in many physiological and pathological processes. Alterations in their levels have been found in many diseases (e.g., neuroinflammatory diseases and metabolic diseases), suggesting a potential therapeutic interest in this class of molecules [9–12]. This is further supported by studies from our group and others, showing that administration of bioactive lipids can have beneficial effects [13–15]. However, direct administration of endocannabinoids can be hampered by their unfavorable properties, such as sensitivity to enzymatic hydrolysis and limited aqueous solubility [16]. We hypothesized that bioactive lipids loading into EV could overcome limitations associated with their administration in the free form [17]. Among bioactive lipids, anandamide (AEA) is particularly representative of these limitations and was therefore selected to investigate the loading of this class of compounds into EV.

In this context, the first objective of this work was to investigate the loading of AEA into EV. We used EV isolated from microglia cells because they produce abundant EV per cell and play an important role in neuroinflammatory disorders, including multiple sclerosis [18]. Our data confirmed the technical challenge of loading therapeutic doses of AEA into EV. The second challenge was the isolation of AEA-loaded EV from saponin and unloaded AEA, a step complicated by the formation of saponin micelles, which hindered the purification process. Finally, we developed a method based on Laurdan fluorescence and generalized polarization (GP) measurements to evaluate how the incorporation of AEA affects EV membrane fluidity.

Materials and methods

Materials

Anandamide (*N*-arachidonoylethanolamine, A0580) was purchased from Sigma-Aldrich (St. Louis, MO, USA). Saponin (558255) was purchased from Calbiochem (KGaA, Darmstadt, Allemagne). Laurdan and Prestoblue Cell Viability Reagent (A13261) were purchased from Thermo Fisher Scientific (Waltham, MA, USA). DMEM (Dulbecco's modified Eagle medium, GlutaMAX, 61965-026), Penicillin-Streptomycin 10,000 U/ml (15140-122), accutase and the BCA protein assay kit (23225) were purchased from Thermo Fisher Scientific (Waltham, MA, USA). Vivaspin6, Centricon70-Plus and Amicon Ultra-0.5 were purchased from Sigma-Aldrich (St. Louis, MO, USA). The size exclusion chromatography (SEC) columns were supplied by Izon (Lyon, France). Rotilabo ® PVDF (polyvinylidene fluoride) 0.22 µm filters were purchased from Carl Roth GmbH (Karlsruhe, Germany). RIPA buffer (ab156034) was purchased from Abcam (Cambridge, UK). Leammli buffer (1610747), 10X Tris/Glycine Buffer (1610771), Any kD Mini-PROTEAN TGX Precast Protein Gels 10-well (4569034) and Trans-blot Turbo Mini 0.2 µm PVDF membrane (1704156) were purchased from Bio-Rad (Hercules, USA). Anti-CD81 (10037) and anti-rabbit IgG HRP-linked antibodies (7074) come from cell signaling Technology (Danvers, USA) and anti-calnexin (ADI-SPA-860) comes from Enzo (NY, USA).

Cell culture

BV2 cells (murine microglial cell line) were routinely cultured at 37 °C in a humidified 5% CO_2 atmosphere in DMEM, supplemented with 1% (v/v) Penicillin-Streptomycin and 10% (v/v) fetal bovine serum (FBS). The medium was replaced 3 times a week.

Production and isolation of EV

EV were isolated following a combination of different methods [19]. When BV2 cells reached 80% of confluency

their medium was changed to FBS-free DMEM medium, supplemented with 1% (v/v) Penicillin-Streptomycin [20]. Then, after 24 h, the medium was collected and successively centrifuged at 300*g for 10 min, 1000*g for 20 min, and 10 000*g for 30 min at 4 °C, to remove cells, dead cells, and cellular debris, respectively. Subsequently, the medium was filtered through a 0.22 µm hydrophilic membrane PVDF (polyvinylidene fluoride) filter (Rotilabo,33 mm) and transferred to a Centricon Plus-70 (regenerated cellulose, NMWL 30,000 Da, UFC703008) and centrifuged at 3000*g for 20 min at 4 °C. The Centricon cup was washed twice with filtered phosphate buffer solution (PBS). Then, EV were collected by centrifugation of the inverted cup at 1000*g for 2 min as per supplier's instructions. The volume was adjusted to reach 500 µl and the solution was loaded on a Size Exclusion Chromatography (SEC) qEV original 35 nm. Filtered PBS was used as eluent, and EV were collected in fractions 7–11 and pooled.

EV characterization

NTA (nanoparticles tracking analysis). Particle concentration and size distribution of EV from BV2 were characterized by NTA (ZetaView Particle Metrix, Inning am Ammersee, Germany).

Protein quantification. EV protein quantification was carried out using BCA protein assay kit, as per the manufacturer's instructions. Briefly, EV were isolated as described in 2.3 and 100 µl of each fraction collected from the SEC were mixed with the BCA reagent before being incubated for 30 min at 37 °C. The absorbance was measured at 562 nm using a spectrophotometer (SpectraMax iD5, Molecular Devices).

Western blot. The protein content of the samples was measured using a BCA Protein assay kit according to the manufacturer's protocol. SDS-PAGE western blotting was performed as follows. Leammli buffer was added to the EV samples in a volume ratio of 1:4 and the samples were heated at 95 °C for 3 min in a water bath. Proteins (9 µg) were loaded in the wells of a 4–20% precast polyacrylamide gel. After electrophoresis (in Tris/Glycine Buffer, 120 V), proteins were electrotransferred onto a PVDF membrane using a Trans-Blot TurboTM transfer system. Membranes were blocked in a 5% BSA TBS buffer (150 mM NaCl, 20 mM Tris) containing 0.1% Tween-20 (TBST) for one hour. Anti-CD81 (dilution: 1/500) and anti-calnexin (dilution: 1/1000, 1%-milk TBST) primary antibodies were incubated overnight at 4 °C and anti-rabbit (dilution: 1/5000, 1%-BSA TBST) secondary antibody was incubated for one hour at room temperature under slow agitation. Membranes were exposed to ECLTM Prime Western Blotting detection reagents (Cytiva, RPN2232) for 5 min and chemoluminescence was visualized using an Amersham ImageQuant 800 western blot imaging system (Cytiva, Chicago, USA).

NanoFCM (nano-flow cytometry). Nano-flow cytometry was performed using the Flow NanoAnalyzer (NanoFCM, UK) following the manufacturer's guidelines. Calibration was carried out with 200 nm PS QC beads (NanoFCM, UK) for particle concentration and S16M-Exo silica beads (NanoFCM, UK) to generate a calibration curve for converting side scatter intensities into particle sizes. The laser configuration included 488 nm and 640 nm lasers at 20 mW, equipped with lens filters at 525/40 and 670/30. For staining, Alexa Fluor® 647-conjugated monoclonal mouse antibodies specific to CD63, CD9, and CD81 (Santa Cruz Biotechnology, USA) were used, along with isotype controls. Antibodies were prepared by centrifugation at 10 000*g for 15 min or filtered through a 0.22 µm syringe filter. Staining was conducted overnight at 4 °C at a 1:10 ratio. Before measurement, labeled vesicles were diluted either 1:50 or 1:20. Positivity was determined using PBS alone, unstained vesicles, isotype controls, and auto-thresholding. The samples were adjusted to 5×10^9 particles/mL for optimal EV staining. Blank controls consisted of PBS and antibodies diluted 100-fold in PBS. To distinguish positive events from background noise in the fluorescence channel, signals from unstained EV and EV with isotype controls were used. Data analysis was performed using NF Profession 1.0 software.

TEM (Transmission Electron Microscopy). To observe EV using TEM, samples underwent a negative staining procedure. A 4 µL aliquot of isolated EV was placed onto copper grids F/C (300 mesh) and left to incubate at room temperature for 5 min. Excess liquid was blotted away with filter paper before staining with 1% uranyl acetate for 20 s at room temperature. After removing the excess stain, the samples were dried and examined with an HT 7700 120 kV (Hitachi, Japan) microscope.

Loading of EV with AEA

EV isolated from BV2 cells (9.10^9 particles in 1 ml of filtered PBS) were loaded with AEA according to different approaches reported in the literature [21–23]. AEA was dissolved in ethanol 99% to obtain a 1 mg/ml stock solution.

Passive incubation. 460 µl of EV were incubated with 4 µl of the AEA stock solution at RT (20 ± 2 °C in our working environment) or 37 °C for 30 or 120 min under agitation (10 rpm).

Saponin-assisted loading. 460 µl of EV were incubated at RT for 30 min under agitation (10 rpm) with 4 µl of the AEA stock solution and with saponin diluted at different concentrations (in water, 0.05%, 0.1%, and 0.2% (w/v)).

Sonication. 460 µl of EV and 4 µl of AEA stock solution were sonicated using an ultrasonic probe (Branson 450 Digital Sonifier) with a 20% amplitude for 6 cycles; each cycle was 30s ON/OFF for 3 min followed by a 2 min cooling period on ice [24].

Isolation of AEA-loaded EV

Two methods were used and compared to separate AEA-loaded EV from saponin and unloaded AEA.

For passive incubation (at RT for 30 min), 460 µl of EV (9.10^9 particles per ml) were incubated with 4 µl of AEA stock solution at 1 mg/ml. For saponin-assisted loading, 460 µl of EV (9.10^9 particles per ml) were incubated with 4 µl of AEA stock solution and with saponin solution (final concentration of 0.2%), at RT for 30 min under agitation (10 rpm). A control condition without EV was also included.

Then the samples were processed by SEC or ultrafiltration (UF). For SEC (qEV Original 35 nm IZON column), 500 µl of the sample was put on the top of the SEC and fractions 7 to 11 were collected by adding filtered PBS. For UF, Amicon Ultra-0.5 NMWL 30 kDa was used as per the manufacturer's instructions. Briefly, samples were added to the filter cup of Amiconwashed twice with 400 µl of filtered PBS (i.e. total washing volume of 800 µl) by centrifugation at 3000*g for 10 min.

For each method, particle concentration, size distribution, and zeta potential were measured by NTA as described in 2.4.

Cytotoxicity on BV2 cells

The samples proceeded as described in 2.6 were diluted in medium (ratio 1:1) and incubated for 24 h with BV2 cells. The media was then removed and replaced with fresh medium containing 10% of PrestoBlue® Cell Viability Reagent. After 1 h of incubation, the fluorescence intensities were measured at RT with a spectrophotometer (SpectraMax iD5, Molecular Devices) using an excitation wavelength (λ_{ex}) of 555 nm and an emission wavelength (λ_{em}) of 595 nm. Untreated BV2 cells were used as the negative control (100% cell viability) and BV2 cells treated with Triton 1% were used as the positive control (10.5% cell viability).

Quantification of AEA by UPLC-MS/MS

The AEA content of the EV was analyzed by UPLC-MS/MS [25]. Briefly, lipids were extracted from the samples by a liquid/liquid extraction (using dichloromethane – methanol – water; 4-2-1; v/v/v) in the presence of the deuterated internal standard (d_4-AEA). Following evaporation of the solvents, the resulting fraction was solubilized in methanol and analyzed using a Xevo-TQS mass spectrometer (from Waters). The samples were separated on a BEH LC-18 column (50*2.1, 1.7 µm; Waters) at a temperature of 40 °C. The mobile phase consisted in a gradient between A: water – methanol (25:75, v/v) and B: methanol 100%, both containing acetic acid (0.1%). An ESI probe operated in positive mode was used for sample ionization. The mass spectrometer parameters were following: capillary voltage: 2.9 kV; cone voltage : 30 V ; desolvation temperature : 550 °C ; desolvation gas flow : 1100 L/Hr : cone gas flow : 170 L/Hr : nebuliser : 6 bar. The transitions followed were 348.2 > 61.9 and 352.2 > 65.9 for AEA and d_4-AEA, respectively. Relative quantification has been obtained by normalization of the area under the curve (AUC) of the AEA using the AUC of d_4-AEA.

Determination of GP value in EV and micelles by using Laurdan

The effect of AEA on the EV membrane fluidity was determined by monitoring the values of generalized polarization (GP) of Laurdan [26]. In preliminary studies, 200 µl of EV (2.10^{10} particles per ml) were incubated with benzyl alcohol (final concentration of 0.34% *(v/v)* or 1.36% *(v/v)*) and a 10 µM Laurdan solution for 60 min under shaking. To explore the effect of AEA and saponin, 200 µl of EV (2.10^{10} particles per ml) were incubated with 4 µl of AEA stock solution and/or saponin solution (final concentration of 0.2%) at RT for 30 min under shaking, before Laurdan addition (final concentration of 10 µM). The samples were then vortexed and incubated at RT for 60 min. The fluorescence intensities were measured at RT with a spectrophotometer (SpectraMax iD5, Molecular Devices) using a fixed excitation wavelength (λ_{ex}) of 340 nm and an emission spectrum between 400 and 600 nm [27]. The GP value was calculated from this equation: $GP = \frac{(I435 - I485)}{(I435 + I485)}$ where I_{435} and I_{485} are the emitted fluorescence intensities measured at 435 and 485 nm, respectively.

Statistics

Student's t-tests and one-way ANOVA were performed using PRISM (Graphpad software, United-States) to determine statistical significance. N indicates the number of independent experiments and n the number of replicates. Information about replicates and statics applied for each experiment can be found in figure captions.

Results

Comparison of different methods for AEA loading in EV

This experiment aimed to compare and select the method providing the highest loading of AEA in EV. Here we compared passive (incubation) and active (physical and chemical) methods.

First, EV were isolated from BV2 cells by SEC (fractions 7–11, Fig. 1A) and characterized to confirm the EV nature of the collected particles. The size distribution (Fig. 1B) and morphology (Fig. 1C) of the particles found in the polled SEC fractions confirmed the presence of EV. Western blot analysis showed that the EV fraction elicited a stronger signal for CD81 (a positive EV marker [28]) compared to the original cells, while the cellular protein marker calnexin was stronger in the cell lysate than in the EV fraction (Fig. 1D). Finally, single-particle analysis by NanoFCM revealed that

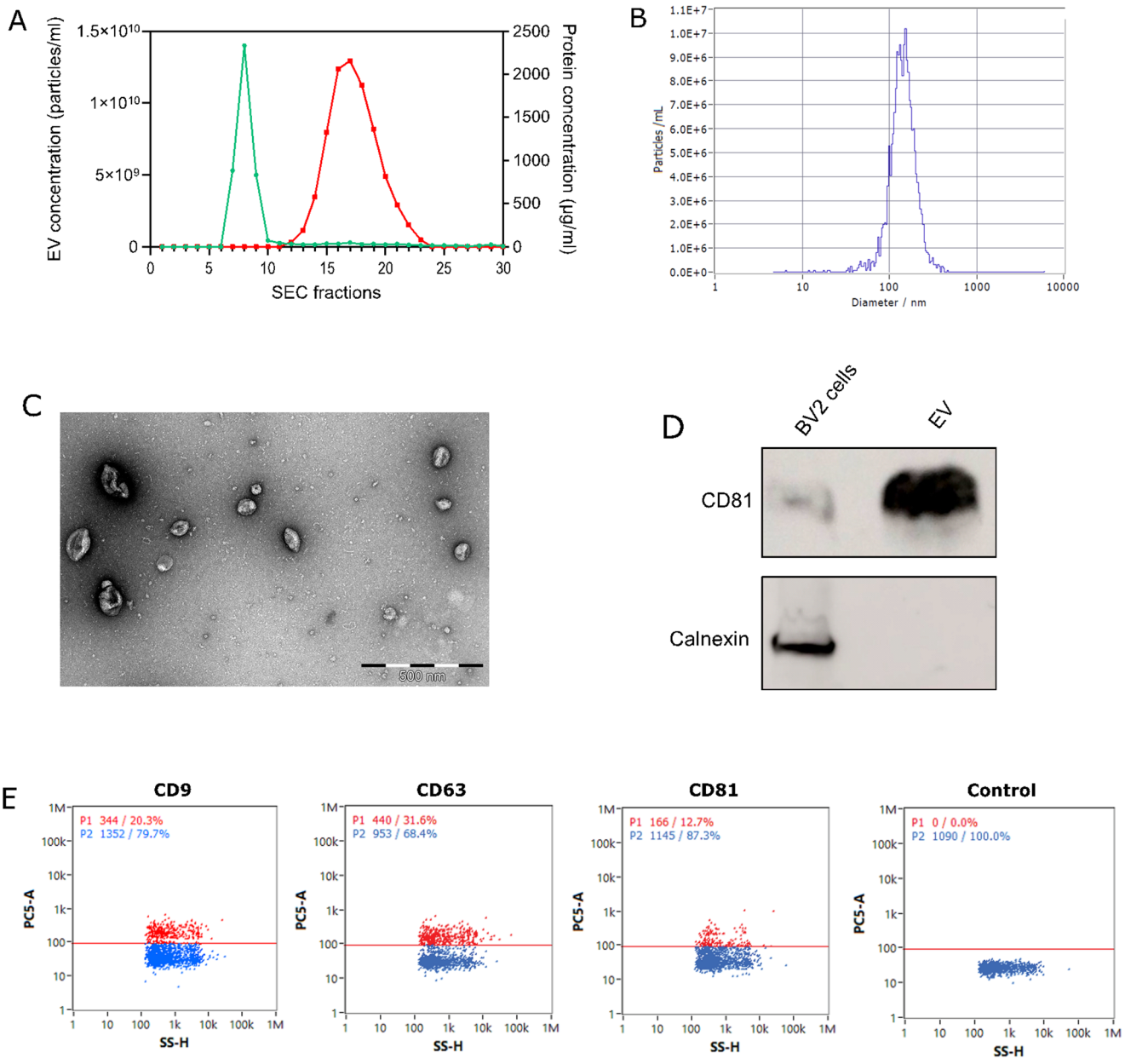

Fig. 1 Characterization of EV from BV2 cell line (**A**) SEC was loaded with 500 µl of EV. 30 fractions were collected and analyzed for particle concentration (green line) and for protein content (red line) by NTA and by BCA assay, respectively. (**B**) Size distribution of the SEC fraction 7–11 (EV) by NTA. (**C**) Representative transmission electron microscopy image of EV (scale bar: 500 nm). (**D**) Western blot analysis of the SEC fraction 7–11 (EV) and of the producing cells (BV2) showing the detection of CD81 (an EV marker) and of the ER-protein calnexin. (**E**) Representative plots of single EV from BV2 expressing CD9, CD63, or CD81 (Tetraspanins; EV markers) by NanoFCM

20.3% of EV measured were positive for CD9, 31.6% for CD63, and 12.7% for CD81 (Fig. 1E).

Next, we tested different approaches to load AEA into EV. First, we evaluated the impact of time (30 versus 120 min) and temperature (RT versus 37 °C). Given the limited effectiveness of the co-incubation, we hypothesized that prolonged incubation time would allow more molecules to diffuse into the EV membrane. Additionally, higher temperatures were expected to modify membrane fluidity and therefore enhance the rate of diffusion. Then, as saponin is largely used to increase EV drug loading [29, 30], we also tested the effect of increasing concentrations of saponin on the loading of AEA into EV. Finally, we assessed the effect of sonication, as this is the most popular physical method to load a drug into EV [24]. The EV suspensions were then ultra-filtrated to remove the unloaded AEA (and saponin when relevant), before quantifying the AEA associated with EV by UPLC-MS/MS.

The highest content of AEA in the EV suspension was found when AEA was incubated with EV in the presence of 0.2% saponin (Fig. 2). The effect of saponin was dose-dependent, with only 0.1% and 0.2% of saponin resulting in a significantly higher amount of AEA (i.e. increased AEA/d_4-AEA ratio) compared to the same condition without saponin (i.e. passive incubation at RT for 30 min). When compared to 30 min incubation at RT, sonication did not increase the amount of AEA detected in the EV suspension.

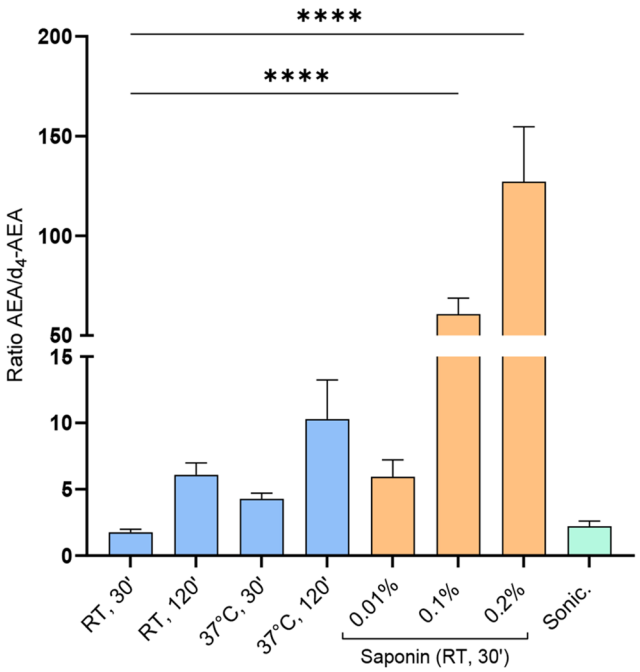

Fig. 2 Impact of the loading method on AEA encapsulation in EV. For passive incubation, AEA was incubated with EV (4.10^9) at RT or 37°C for 30 or 120 min (blue bars). Alternatively, the incubation (RT, 30 min) was performed in the presence of increasing concentrations of saponin, from 0.01% to 0.2% (orange bars), or incubation of AEA and EV was sonicated (green bar). AEA was then quantified by UPLC-MS/MS in the presence of d_4-AEA as IS. The signal detected for AEA was normalized with the signal of the IS and the data was reported as mean ± SEM (N= 3, n=3). Statistical significance was determined by Dunn's test *p≤ 0.5

Isolation of AEA-loaded EV

Although the saponin-assisted method was the one providing the highest signal for AEA (reported here as ratio between AEA and the internal standard d_4-AEA), saponin is cytotoxic, as confirmed here for BV2 cells at saponin concentrations ranging from 0.2 to 0.01% (Fig. 3), and thus, must be completely removed from the EV suspension after AEA loading [4, 6, 30].

Hence, we compared SEC and UF [31] to isolate AEA-loaded EV and eliminate saponin from the AEA-loaded EV suspension. The impact of EV suspensions (i.e. fractions 7–11 from SEC and concentrate after UF) on the viability of BV2 cells was assessed (Fig. 4B). When EV were incubated with AEA (passive incubation), no significant differences were observed compared to the untreated BV2 cells (medium), regardless of the isolation method used. EV incubated with AEA and saponin (saponin-assisted loading), and isolated using SEC, did not significantly decrease BV2 cell viability. In contrast, EV incubated with AEA and saponin, and processed by UF, dramatically dropped the BV2 cell viability to 9%. AEA incubated with saponin (in the absence of EV) was used as a negative control and cytotoxicity was observed after processing it on UF (11% cell viability), but not after SEC.

To further compare the different procedures, EV number and size, which inform on the potential loss of particles or their alteration, as well as the AEA content associated with EV were analyzed. When EV were incubated with AEA (passive incubation), the highest number of particles was observed after purification by SEC (Fig. 4D). In both isolation methods, the addition of saponin did not significantly change the number of particles recovered. AEA incubated with saponin (in the absence of EV) was used as a negative control and no particles were expected to be detected in this condition. However, although to a lesser extent than in the presence of EV, particles were detected in this condition, regardless of the isolation method. The size of the particles collected was between 119 nm and 136 nm (Fig. 4C).

When analyzing the amount of AEA in the EV suspensions (i.e. fractions 7–11 from SEC and concentrate from UF) by UPLC-MS/MS, we found that AEA levels were significantly lower after SEC compared to UF (Fig. 4E). Consistent with data presented above (Fig. 2), the AEA content increased in the presence of saponin 0.2% when using UF. AEA was detected in the negative control (i.e. AEA incubated with saponin in the absence of EV) at the same ratio

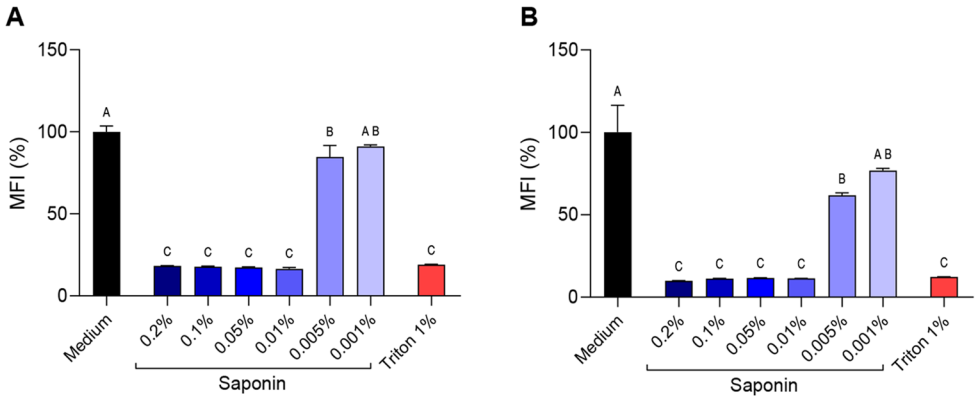

Fig. 3 Cells viability of BV2 incubated with different concentrations of saponin. BV2 cells (10^5 cells/well) were seeded in a 96-well plate overnight. Then, cells were incubated for 8 h (**A**) or 24 h (**B**) with saponin (from 0.001 to 0.2%), or with 1% Triton (used as positive control). A condition with medium only was used as a negative control. Afterward, cells were incubated for 1 h with the resazurin-based PrestoBlueTM reagent to assess cell viability. The mean fluorescence intensity (MFI, relative to the negative control) was measured at 560/590 nm using a SpectraMax® ID5. The values were represented as mean ± SEM ($N = 1$, $n = 4$). One-way ANOVA, Tukey's multiple comparison test among all groups. Conditions not linked with the same letter are statistically different ($p < 0.0001$)

as in the condition containing EV. Using UF, we observed that the particle count was lower when AEA was incubated with saponin alone compared to incubation with both EV and saponin. However, the amount of AEA remained similar in both conditions (Fig. 4D and E).

Co-isolation of saponin micelles with AEA-loaded EV

The detection of a significant amount of AEA in the presence of saponin, in the absence of EV, was striking. We hypothesized that saponin formed micelles (with the same size range as EV) in which AEA was encapsulated. Indeed, in aqueous solutions and at a concentration above the critical micellar concentration (CMC), saponin forms amphiphilic aggregates called micelles. The CMC varies depending on the origin of the saponin, ranging from 0.001 to 0.077% (62). In this study, we used a commercially available saponin made of a mixture of saponins from various plants, so the theoretical CMC was unknown. The experimental CMC we determined by using Hoechst dye was equal to 0.043 ± 0.004%, way below the concentration used in our experiments (0.2%) (Fig. 5) [32].

When the concentration of the saponin in the solution increased, the number of particles detected by NTA increased too (Fig. 6A). Their size distribution was very heterogeneous, much more than for the EV suspension (data not shown). Moreover, particles detected in the saponin solutions had a similar size as EV isolated from BV2 cells (Fig. 6B).

Impact of EV incubation with AEA and saponin on the EV membrane

Given the lipophilic properties of AEA, we hypothesized that the AEA associated with EV may have inserted into their membrane. To explore this possibility, the effect of AEA, as well as saponin, on EV membrane fluidity was studied using the fluorescent probe Laurdan [26, 33]. Variations in membrane fluidity, as reflected by changes in the GP value, would suggest a shift in the phase state of the membrane (from ordered to disordered state, or inversely), which could be attributed to the insertion of AEA into the EV membrane.

Although this method is routinely used for cells and synthetic nanoparticles, it has not been widely used to study EV membrane properties [26, 34]. Therefore, our first objective was to optimize the experimental conditions for determining the GP of EV membrane. To validate the applicability of the Laurdan method to EV, we first determined GP values of EV at different temperatures. The GP values ranged between 0.04 and 0.08, and remained stable across the tested temperature range, suggesting that temperature does not significantly affect the Laurdan signal in EV membranes (Fig. 7A).

To further confirm the sensitivity of the method to variations in membrane fluidity, we incubated EV with a known biological membrane fluidizer, namely benzyl alcohol [35]. According to the literature, benzyl alcohol disrupts lipid packing and increases membrane fluidity over a broad concentration range. We tested two concentrations of benzyl alcohol (0.34% and 1.36%) and observed that even the lower concentration was sufficient to significantly decrease GP values, as expected from this membrane fluidizer (Fig. 7B).

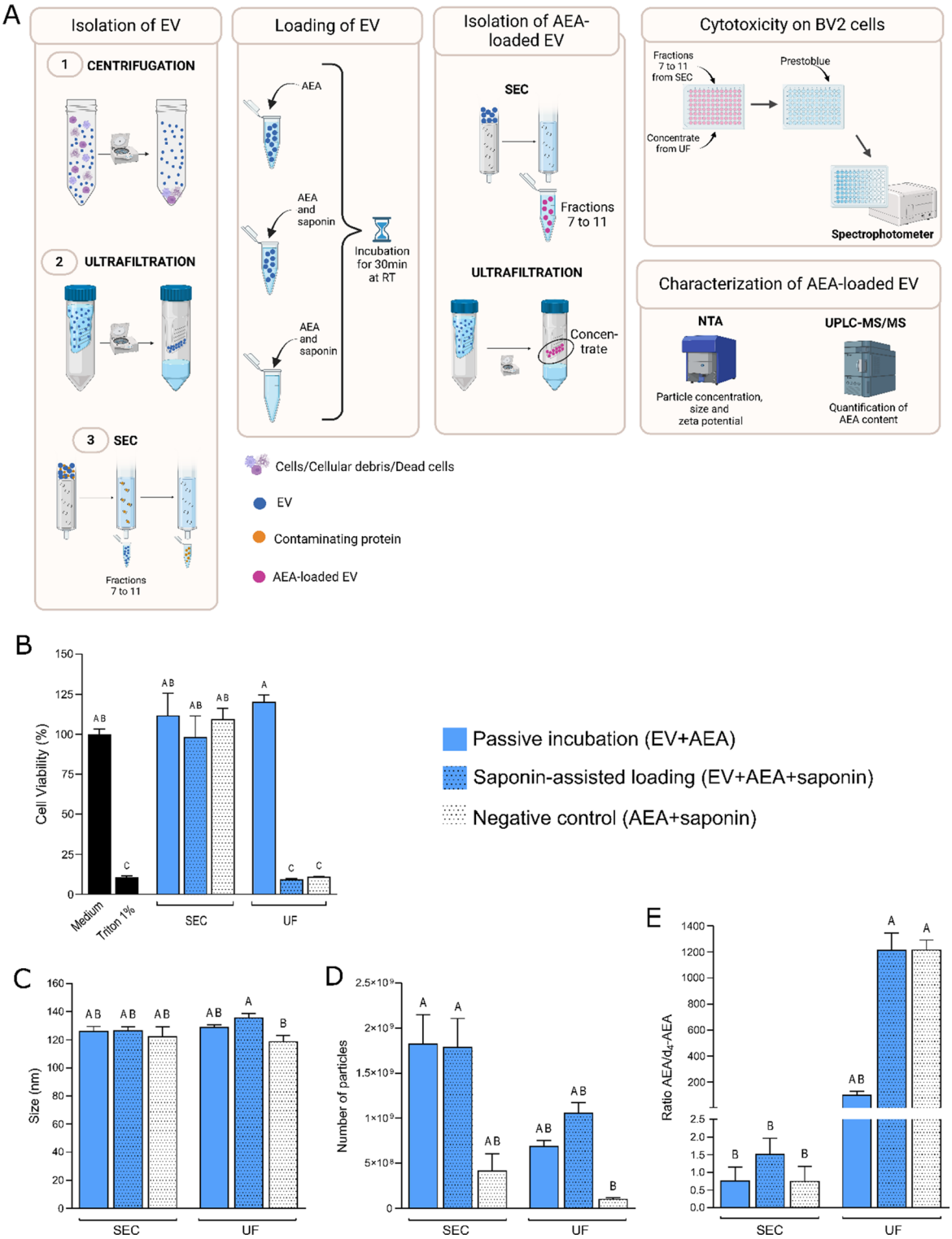

Fig. 4 Impact of the isolation method on cytotoxicity, size and particle number, and on AEA loading (**A**) EV were isolated from BV2 cells for loading (cfr 2.3):(1) cells/cell debris/dead cells were pelleted by centrifugation(2)the EV suspension was concentrated by UF(3) EV were passed through SEC to remove contaminating proteins. AEA was incubated with EV suspension (4.10^9 particles) in the absence or presence of saponin (final concentration of 0.2%). AEA was also incubated with saponin (final concentration of 0.2%) in the absence of EV. Following incubation (30 min, RT), EV were isolated by SEC or UF. Finally, fractions 7 to 11 (from SEC) and concentrate (from UF device) were collected, and (**B**) incubated with BV2 cells for 24 h to evaluate their cytotoxicity via PrestoBlueTM reagent. Fractions 7 to 11 and concentrate were also characterized. (**C**) The size and (**D**) the total number of particles was measured by NTA. (**E**) AEA was quantified by UPLC-MS/MS in the presence of d_4-AEA as IS. The signal detected for AEA was normalized with the signal of the IS. The values were reported as the mean ± SEM ($N=3$, $n=3$). Statistical significance was determined by a Kruskal-Wallis test

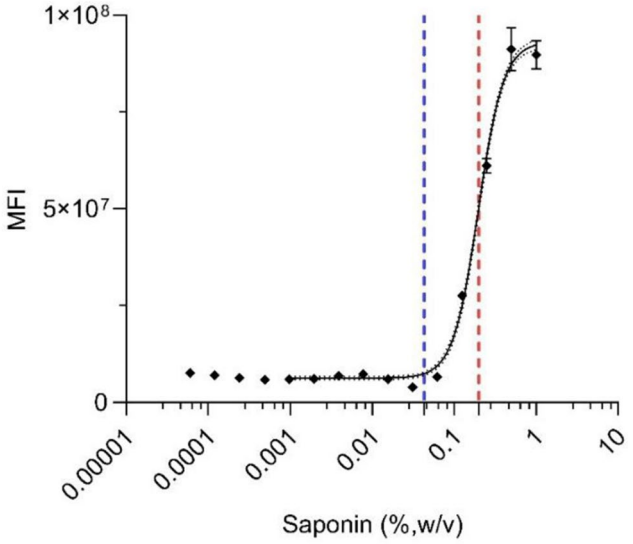

Fig. 5 Formation of micelles in saponin solutions. The CMC of our saponin batch was determined using the Hoechst dye (vertical blue line). Hoechst (final concentration of 7μM) was added to different saponin solutions (serial dilutions of 1% stock solution). The mean fluorescence intensity (MFI) was measured at 355/460 nm using a SpectraMax ® ID5. The vertical red line represents the concentration of saponin used in our experiments (0.2%). The values were represented as mean ± SEM (N=3, n=4)

Next, the impact of AEA on EV membrane fluidity was assessed in 3 conditions: (1) EV incubated with AEA ,(2), EV incubated with AEA and saponin, as saponin interacts with membranes (3), and AEA incubated with saponin, as our data strongly suggested an association between AEA and saponin. AEA significantly decreased the GP value of EV while it increased the GP value of saponin micelles (although the change in GP value was not statistically significant) (Fig. 8). It is interesting to note that AEA still decreased the GP value of EV in the presence of saponin, but to a lesser extent than in EV alone.

Discussion

An increasing number of studies, including from our lab, support the therapeutic potential of bioactive lipids, particularly in the context of inflammatory diseases [36]. Unfortunately, unfavorable physicochemical properties and/or poor enzymatic stability hinder their administration in free form. These limitations may be overcome by encapsulating bioactive lipids into nanoparticles [37]. In recent years, EV have attracted scientific interest as innovative drug carrier systems. However, a major challenge when using EV as nanocarriers is reaching drug loading concentrations that are therapeutically relevant. The mechanisms involved in cargo loading into EV are still not sufficiently understood, and the efficiency of the loading method depends on several experimental factors [38]. Although multiple strategies have been developed to improve drug loading into EV, only a few have specifically addressed the loading of bioactive lipids [39].

Among all loading methods tested, incubation with saponin (final concentration of 0.1% and 0.2%) resulted in the highest levels of AEA. This well-referenced and widespread method is known to increase membrane permeability by forming pores via the complexation of saponin with cholesterol in the EV lipid bilayer, allowing the entry or intercalation of exogenous molecules [33]. Saponin, at concentrations ranging from 0.01 to 0.2%, has been reported to increase the loading efficiency of doxorubicin, porphyrin, or proteins such as TRP2 peptide or catalase, into EV [21–23, 40, 41].

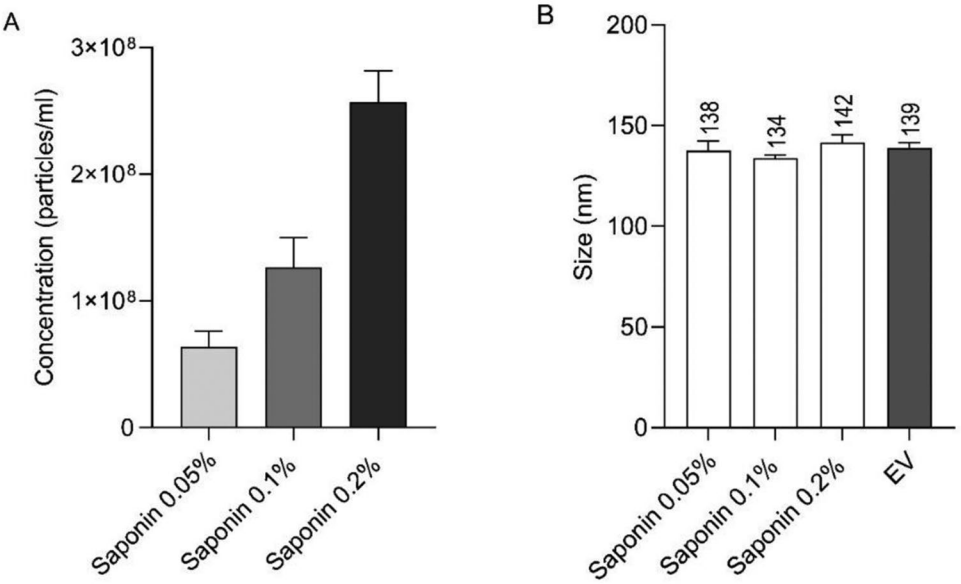

Fig. 6 Formation of micelles in saponin solution. (**A**-**B**) Saponin solutions were prepared in filtered PBS, reaching a final concentration of 0.05%, 0.1% and 0.2%. (**A**) Particle concentration (particles/ml) and (**B**) size (nm) were measured by NTA at RT. The values were presented as mean ± SEM ($N=3$, $n=3$)

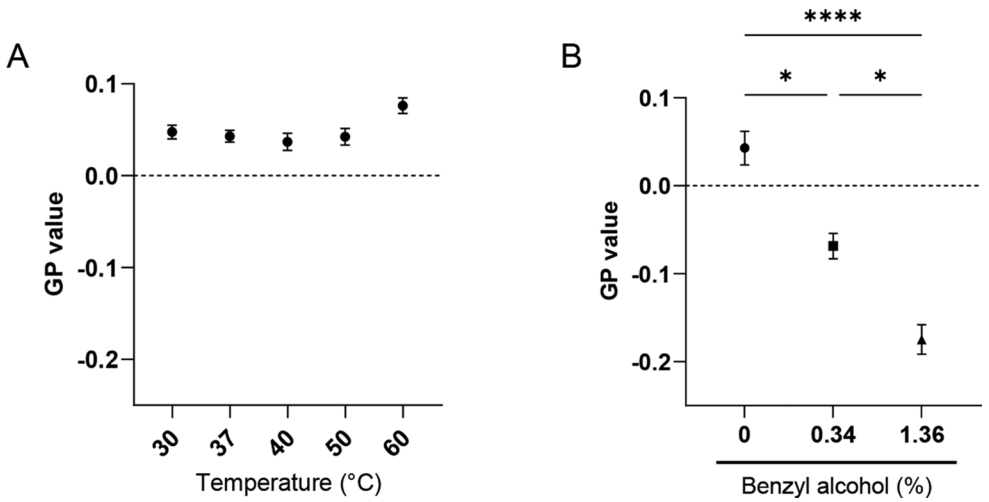

Fig. 7 GP values of Laurdan in EV according to different temperatures, with or without benzyl alcohol. (**A**) EV (4.10^9) were incubated with Laurdan 10 µM (final concentration) at RT for 60 min. Laurdan generalized polarization (GP) was assessed at multiple temperatures from 30° to 60 °C. (**B**) EV (4.10^9) were incubated with Laurdan 10 µM (final concentration) in the absence (round) or the presence of benzyl alcohol at 0.34% (square) and 1.36% (triangle). The incubation was performed at 37 °C for 60 min. GP was assessed at 37 °C. The values were represented as mean ± SEM ($N = 3$, $n = 3$). Statistical significance was determined by a Dunn's test *p ≤ 0.5

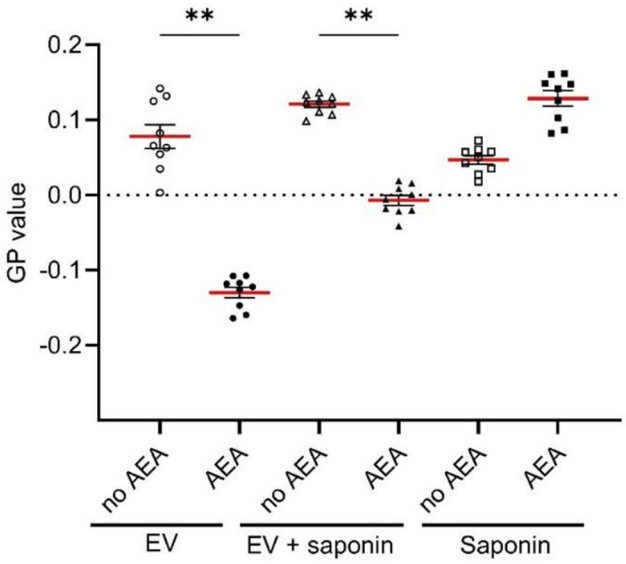

Fig. 8 Impact of AEA on the membranes of EV and saponin micelles EV (4.10^9), saponin (final concentration of 0.2%) and both EV and saponin (4.10^9 and 0.2%, respectively) were incubated without (empty symbols) or with (filled symbols) AEA for 30 min at RT, before Laurdan addition (10 µM). Laurdan generalized polarization (GP) was assessed at RT after 60 min of incubation. The more positive the GP, the more ordered the membrane, and the more negative the GP, the more disordered the membrane. The results were expressed as the mean ± SEM ($N = 3$, $n = 3$). Statistical significance was determined by a Dunnett test *p ≤ 0.5

However, a critical step following the saponin-assisted method is the separation of drug-loaded EV from saponin, due to its well-known cytotoxicity [5, 6, 42]. Additionally, in the context of EV-based nanocarriers, separating drug-loaded EV from unloaded drugs is essential to enhance process reproducibility, consistency in the administered dose, and reliable data interpretation [43].

Several post-loading isolation methods have been described in the literature, including ultracentrifugation, sucrose gradient centrifugation, column chromatographic separation, UF, and exosome isolation kits [43]. The optimal choice depends on parameters such as the nature of the drug and EV, the loading approach used, and the practical aspects of implementation. Although ultracentrifugation is the most commonly used technique, the mechanical stress can induce EV aggregation and leakage of the loaded drug from EV [44]. Therefore, SEC and UF were selected as alternative methods. SEC separates components based on size: small molecules, such as unloaded AEA and saponin monomers, are retained in the porous beads, while EV are eluted faster and collected in the earlier fractions [45]. UF relies on semi-permeable membranes with predetermined pore sizes that retain larger particles (EV) and allow smaller molecules (unloaded AEA and saponin monomers) to pass through.

The choice of post-loading isolation method proved critical, as we found that AEA-loaded EV were toxic for cells after passing through UF, but not after SEC (Fig. 4B). This suggests that higher doses of residual saponin remained in AEA-loaded EV suspension following UF. The underlying mechanisms of these two isolation methods may explain the lower efficiency of UF in removing saponin. In SEC, sample components strongly interact with the porous stationary phase, allowing the elimination of both free saponin in the aqueous phase and saponin loosely associated with the EV surface. In contrast, UF relies on the passive diffusion of small free molecules (free AEA and saponin monomers) through the semi-permeable membrane, and multiple

washings are required to dilute and progressively eliminate free molecules.

In addition, the post-loading isolation method significantly influenced the amount of AEA detected in the EV suspension. Specifically, higher AEA levels were detected after UF than after SEC. We hypothesized that this gap is due to the formation of saponin micelles in which AEA is trapped. Saponin is amphiphilic and can self-assemble into micelles when used above its critical micellar concentration (CMC). The concentration of saponin we used in our experiments (0.2%) was approximately five times higher than its CMC (0.043%), thus favoring the formation of micelles. Moreover, at saponin concentrations below the CMC (0.01%) (Fig. 2), AEA levels did not significantly differ from those observed with passive incubation (at RT for 30 min), supporting a real impact of saponin micelles formation on data interpretation.

To further investigate this, we calculate the AEA-to-particle ratio (AEA/d_4-AEA signal normalized to particle number measured by NTA) following incubation of AEA with either EV alone (passive incubation) or saponin alone (negative control) (Fig. 4). We found that the AEA-to-particle ratio was nearly 100 times higher after incubation with saponin than with EV. This finding is consistent with the distinct loading mechanisms: saponin micelles form spontaneously around AEA, whereas EV are pre-formed vesicles that require diffusion-based cargo incorporation, a less efficient process.

Altogether, saponin was identified here as a confounding factor when evaluating the encapsulation of a bioactive lipid in EV, highlighting the importance of implementing rigorous controls and selecting an appropriate purification method. Moreover, saponin hemolytic properties, which can lead to anemia and potentially death [33], raise safety concerns for downstream applications. Therefore, passive incubation, which is the method providing the highest AEA loading in the absence of saponin, was selected for future formulations of AEA-loaded EV. To address translational considerations, the stability of AEA-loaded EV was evaluated following multiple freeze-thaw cycles (Supplemental Figure S1) and storage at -80 °C versus 4 °C for 1 and 2 weeks (Supplemental Figure S2), by measuring their particle concentration, size, ZP and AEA content. While repeated freeze-thaw cycles affected only particle concentration, the storage duration had an impact on particle concentration, ZP and AEA content, regardless of the temperature.

In addition to evaluating loading efficiency, understanding the localization of AEA within the EV is essential. Whether the bioactive molecule resides within the EV lumen or integrates into the membrane (or both) largely depends on its physicochemical properties. Hydrophilic molecules tend to accumulate in the lumen, while hydrophobic molecules tend to associate with the lipid bilayer [45, 46]. Given its lipophilic nature, we expected AEA to be preferentially loaded into the EV membrane. To investigate this, we used Laurdan and measured of Generalized Polarization (GP) value. Laurdan is a polarity-sensitive fluorescent probe that anchors in the phospholipid bilayer, with its lauric acid tail aligning with the lipid acyl chains. Upon excitation, Laurdan generates a strong dipole that interacts with surrounding water molecules. These interactions cause a shift in its emission spectrum, which reflects the phase of the membrane: increased water penetration in disordered (liquid-crystalline) phases, and limited water penetration in ordered phases. We hypothesize that if AEA intercalates into the EV membrane, changes in membrane fluidity will result [47]. While this technique is widely used to study biological and artificial membranes, such as cells and liposomes, respectively [48], its application to EV is still rare. Very few studies have used Laurdan to investigate the membrane fluidity of EV, and even fewer report its use to address the integration of molecules in EV membrane. Our data (Fig. 7A et B) support the robustness of the Laurdan method for detecting changes in EV membrane fluidity.

Our data show a consistent decrease in GP values upon AEA addition, regardless of the presence of saponin, probably reflecting the AEA interactions with EV membrane. This observation is in line with the work of Di Scala et al., who suggested that AEA interacted with cholesterol present in cell membrane by the formation of a hydrogen bond (between the -OH group of the sterol and the -NH group of the AEA), followed by van der Waals interactions and a conformational shift of AEA from a hairpin to an extended form [49]. Although the percentage of cholesterol in membranes depends on the donor cell, EV are enriched in cholesterol compared to their donor cells [50], with levels exceeding 40% of total lipid content in most cases [51]. Harris and his colleagues previously reported that increasing cholesterol content in dipalmitoylphosphatidylcholine liposomes attenuates the thermal phase transition from gel to liquid [48]. Our data show no detectable phase transition from gel to liquid phase upon temperature increase (Fig. 7A), consistent with the presence of high cholesterol levels in EV isolated from BV2 cells.

Assuming that both saponin and AEA interact with cholesterol in the membrane, there is probably a competition for their incorporation into the EV membrane. This hypothesis is supported by our observation that the combination of AEA and saponin induced a smaller change in GP values compared to AEA alone (Fig. 8), suggesting that saponin may partially block AEA insertion by occupying cholesterol-rich regions of the membrane.

Conclusion

In summary, with the aim of loading a bioactive lipid into EV, we compared the efficiency of different loading methods for encapsulating AEA. The saponin-assisted method provided the highest AEA signal compared to passive incubation and sonication. Afterward, two purification methods, SEC and UF, were compared to separate AEA-loaded EV from saponin and unloaded AEA. We found that the formation of saponin micelles (1) prevents the complete elimination of saponin from AEA-loaded EV when using UF, and (2) competes with EV for AEA encapsulation.

This study highlights several key considerations for the field: the challenges of loading a bioactive lipid into EV, the importance of distinguishing between actual drug-loaded EV and drug-loaded micelles, and the need to develop alternative purification methods. Moreover, this study demonstrates that Laurdan technique, not widely applied in the EV field, offers a promising strategy to characterize molecule incorporation into EV membrane.

All together, these insights contribute to the broader understanding of EV as drug delivery systems, particularly for lipophilic therapeutic agents like endocannabinoids, and lay the foundation for future studies aimed at improving the delivery of bioactive lipids via EV.

Supplementary Information The online version contains supplementary material available at https://doi.org/10.1007/s13346-025-01951-4.

Acknowledgements Anne des Rieux is an Honorary F.R.S.-FNRS Senior Research Associate. This work has been supported by the Communauté Française de Belgique in the scope of actions de recherche concertées (ARC) and the Université catholique de Louvain. The Belgian Charcot Foundation is also acknowledged for supporting AdR and GGM research. We would also like to thank Doriane Frederic for providing us with primary antibodies.

Author contributions Marie Auquière performed conceptualization, methodology, investigation, data collection, visualization, and writing of the original draft. Romano Terrasi, Viridiane Gratpain, Jessica Vanderstreaten, Negar Mozaheb contributed to the methodology and investigation. Marie-Paule Mingeot-Leclercq contributed to the methodology and writing – review and editing. Anne des Rieux and Giulio Muccioli performed conceptualization, funding acquisition, visualization, supervision, and writing – review and editing.

Funding I confirm that I have mentioned all organizations that funded my research in the Acknowledgements section of my submission, including grant numbers where appropriate.

Data availability The datasets generated during and/or analyzed during the current study are available from the corresponding author on reasonable request.

Declarations

Ethical approval This study did not involve human or animal subjects. This study did not require ethics approval.

Consent to participate This study did not involve human participation. This study did not require consent to participate.

Competing interests The authors have no relevant financial or non-financial interests to disclose.

Consent to publish This study did not contain any individual person's data. This study did not require consent to publish.

Geolocalisation information Europe, Belgium, Brussels.

References

1. Perocheau D, Touramanidou L, Gurung S, Gissen P, Baruteau J. Clinical applications for exosomes: are we there yet? Br J Pharmacol. 2021;178(12):2375–92. https://doi.org/10.1111/bph.15432.
2. Chen H, Wang L, Zeng X, Schwarz H, Nanda HS, Peng X, et al. Exosomes, a new star for targeted delivery. Front Cell Dev Biol. 2021;9:751079. https://doi.org/10.3389/fcell.2021.751079.
3. Kim HI, Park J, Zhu Y, Wang X, Han Y, Zhang D. Recent advances in extracellular vesicles for therapeutic cargo delivery. Exp Mol Med. 2024;56(4):836–49. https://doi.org/10.1038/s12276-024-01201-6.
4. Das CK, Jena BC, Banerjee I, Das S, Parekh A, Bhutia SK, et al. Exosome as a novel shuttle for delivery of therapeutics across biological barriers. Mol Pharm. 2019;16(1):24–40. https://doi.org/10.1021/acs.molpharmaceut.8b00901.
5. Herrmann IK, Wood MJA, Fuhrmann G. Extracellular vesicles as a next-generation drug delivery platform. Nat Nanotechnol. 2021;16(7):748–59. https://doi.org/10.1038/s41565-021-00931-2.
6. Zhang Y, Bi J, Huang J, Tang Y, Du S, Li P, Exosome. A review of its classification, isolation techniques, storage, diagnostic and targeted therapy applications. Int J Nanomed. 2020;15:6917–34. https://doi.org/10.2147/IJN.S264498.
7. Jang YJ, Cha BS, Kim D, Lee ES, Kim S, Han J, et al. Extracellular vesicles, as drug-delivery vehicles, improve the biological activities of Astaxanthin. Antioxid (Basel). 2023;12(2). https://doi.org/10.3390/antiox12020473.
8. de Escude Martinez P, Tong L, Huang C, Sofias AM, Pastorin G, Chen X, et al. Extracellular vesicles as a drug delivery system: A systematic review of preclinical studies. Adv Drug Deliv Rev. 2021;175:113801. https://doi.org/10.1016/j.addr.2021.05.011.
9. Guillemot-Legris O, Muccioli GG. The oxysterome and its receptors as Pharmacological targets in inflammatory diseases. Br J Pharmacol. 2022;179(21):4917–40. https://doi.org/10.1111/bph.15479.
10. Gustavsen S, Olsson A, Oturai AB, Linnet K, Thomsen R, Rasmussen BS, et al. The peripheral endocannabinoid system and its association with biomarkers of inflammation in untreated patients with multiple sclerosis. Eur J Neurol. 2023;30(10):3212–20. https://doi.org/10.1111/ene.15930.
11. Novakova L, Singh AK, Axelsson M, Stahlman M, Adiels M, Malmestrom C, et al. Sulfatide isoform pattern in cerebrospinal fluid discriminates progressive MS from relapsing-remitting MS. J Neurochem. 2018;146(3):322–32. https://doi.org/10.1111/jnc.14452.

12. Broos JY, Loonstra FC, de Ruiter LRJ, Gouda M, Fung WH, Schoonheim MM, et al. Association of arachidonic Acid-Derived lipid mediators with disease severity in patients with relapsing and progressive multiple sclerosis. Neurology. 2023;101(5):e533–45. https://doi.org/10.1212/WNL.0000000000207459.
13. Miranda J, Brazil JC, Morris AH, Parkos CA, Quiros M, Nusrat A. Maresin-2 promotes mucosal repair and has therapeutic potential when encapsulated in thermostable nanoparticles. Proc Natl Acad Sci U S A. 2023;120(4):e2218162120. https://doi.org/10.1073/pnas.2218162120.
14. Buisseret B, Guillemot-Legris O, Muccioli GG, Alhouayek M. Prostaglandin D(2)-glycerol ester decreases carrageenan-induced inflammation and hyperalgesia in mice. Biochim Biophys Acta Mol Cell Biol Lipids. 2019;1864(5):609–18. https://doi.org/10.1016/j.bbalip.2019.01.009.
15. Alhouayek M, Ameraoui H, Muccioli GG. Bioactive lipids in inflammatory bowel diseases - From pathophysiological alterations to therapeutic opportunities. Biochim Biophys Acta Mol Cell Biol Lipids. 2021;1866(2):158854. https://doi.org/10.1016/j.bbalip.2020.158854.
16. Rohrig W, Achenbach S, Deutsch B, Pischetsrieder M. Quantification of 24 Circulating endocannabinoids, endocannabinoid-related compounds, and their phospholipid precursors in human plasma by UHPLC-MS/MS. J Lipid Res. 2019;60(8):1475–88. https://doi.org/10.1194/jlr.D094680.
17. Martin Gimenez VM, Diaz-Rodriguez P, Sanz RL, Vivero-Lopez M, Concheiro A, Diez E, et al. Anandamide-nanoformulation obtained by electrospraying for cardiovascular therapy. Int J Pharm. 2019;566:1–10. https://doi.org/10.1016/j.ijpharm.2019.05.047.
18. Yong VW. Microglia in multiple sclerosis: protectors turn destroyers. Neuron. 2022;110(21):3534–48. https://doi.org/10.1016/j.neuron.2022.06.023.
19. Gratpain V, Loriot A, Bottemanne P, d'Auria L, Terrasi R, Payen VL, et al. Influence of a pro-inflammatory stimulus on the MiRNA and lipid content of human dental stem cell-derived extracellular vesicles and their impact on microglial activation. Heliyon. 2024;10(5):e27025. https://doi.org/10.1016/j.heliyon.2024.e27025.
20. Wang F, Cerione RA, Antonyak MA. Isolation and characterization of extracellular vesicles produced by cell lines. STAR Protoc. 2021;2(1):100295. https://doi.org/10.1016/j.xpro.2021.100295.
21. Haney MJ, Klyachko NL, Zhao Y, Gupta R, Plotnikova EG, He Z, et al. Exosomes as drug delivery vehicles for parkinson's disease therapy. J Control Release. 2015;207:18–30. https://doi.org/10.1016/j.jconrel.2015.03.033.
22. Goh WJ, Lee CK, Zou S, Woon EC, Czarny B, Pastorin G. Doxorubicin-loaded cell-derived nanovesicles: an alternative targeted approach for anti-tumor therapy. Int J Nanomed. 2017;12:2759–67. https://doi.org/10.2147/IJN.S131786.
23. Fuhrmann G, Serio A, Mazo M, Nair R, Stevens MM. Active loading into extracellular vesicles significantly improves the cellular uptake and photodynamic effect of porphyrins. J Control Release. 2015;205:35–44. https://doi.org/10.1016/j.jconrel.2014.11.029.
24. Salarpour S, Forootanfar H, Pournamdari M, Ahmadi-Zeidabadi M, Esmaeeli M, Pardakhty A. Paclitaxel incorporated exosomes derived from glioblastoma cells: comparative study of two loading techniques. Daru. 2019;27(2):533–9. https://doi.org/10.1007/s40199-019-00280-5.
25. Paquot A, Bestard-Escalas J, Muccioli GG. Set up and validation of a sensitive method to quantify prostaglandins, prostaglandin-glycerol esters and prostaglandin-ethanolamides, as well as their respective precursors. Prostaglandins Other Lipid Mediat. 2023;168:106763. https://doi.org/10.1016/j.prostaglandins.2023.106763.
26. Suga K, Matsui D, Watanabe N, Okamoto Y, Umakoshi H. Insight into the Exosomal membrane: from viewpoints of membrane fluidity and Polarity. Langmuir. 2021;37(38):11195–202. https://doi.org/10.1021/acs.langmuir.1c00687.
27. Parasassi TDSG, Ravagnan G, Rusch M, Gratton R. Quantitation of lipid phases in phospholipid vesicles by the generalized polarization of Laurdan fluorescence. Biophys J Biophys Soc. 1991;60:179–89.
28. Thery C, Witwer KW, Aikawa E, Alcaraz MJ, Anderson JD, Andriantsitohaina R, et al. Minimal information for studies of extracellular vesicles 2018 (MISEV2018): a position statement of the international society for extracellular vesicles and update of the MISEV2014 guidelines. J Extracell Vesicles. 2018;7(1):1535750. https://doi.org/10.1080/20013078.2018.1535750.
29. Han Y, Jones TW, Dutta S, Zhu Y, Wang X, Narayanan SP, et al. Overview and update on methods for cargo loading into extracellular vesicles. Processes (Basel). 2021;9(2). https://doi.org/10.3390/pr9020356.
30. Luan X, Sansanaphongpricha K, Myers I, Chen H, Yuan H, Sun D. Engineering exosomes as refined biological nanoplatforms for drug delivery. Acta Pharmacol Sin. 2017;38(6):754–63. https://doi.org/10.1038/aps.2017.12.
31. Bunggulawa EJ, Wang W, Yin T, Wang N, Durkan C, Wang Y, et al. Recent advancements in the use of exosomes as drug delivery systems. J Nanobiotechnol. 2018;16(1):81. https://doi.org/10.1186/s12951-018-0403-9.
32. Jumpertz T, Tschapek B, Infed N, Smits SH, Ernst R, Schmitt L. High-throughput evaluation of the critical micelle concentration of detergents. Anal Biochem. 2011;408(1):64–70. https://doi.org/10.1016/j.ab.2010.09.011.
33. Lorent JH, Quetin-Leclercq J, Mingeot-Leclercq MP. The amphiphilic nature of saponins and their effects on artificial and biological membranes and potential consequences for red blood and cancer cells. Org Biomol Chem. 2014;12(44):8803–22. https://doi.org/10.1039/c4ob01652a.
34. Simbari F, McCaskill J, Coakley G, Millar M, Maizels RM, Fabrias G, et al. Plasmalogen enrichment in exosomes secreted by a nematode parasite versus those derived from its mouse host: implications for exosome stability and biology. J Extracell Vesicles. 2016;5:30741. https://doi.org/10.3402/jev.v5.30741.
35. Shigapova N, Torok Z, Balogh G, Goloubinoff P, Vigh L, Horvath I. Membrane fluidization triggers membrane remodeling which affects the thermotolerance in Escherichia coli. Biochem Biophys Res Commun. 2005;328(4):1216–23. https://doi.org/10.1016/j.bbrc.2005.01.081.
36. Bottemanne P, Muccioli GG, Alhouayek M. N-acylethanolamine hydrolyzing acid amidase inhibition: tools and potential therapeutic opportunities. Drug Discov Today. 2018;23(8):1520–9. https://doi.org/10.1016/j.drudis.2018.03.007.
37. Mwema A, Bottemanne P, Paquot A, Ucakar B, Vanvarenberg K, Alhouayek M, et al. Lipid nanocapsules for the nose-to-brain delivery of the anti-inflammatory bioactive lipid PGD(2)-G. Nanomedicine. 2023;48:102633. https://doi.org/10.1016/j.nano.2022.102633.
38. Hussen BM, Faraj GSH, Rasul MF, Hidayat HJ, Salihi A, Baniahmad A, et al. Strategies to overcome the main challenges of the use of exosomes as drug carrier for cancer therapy. Cancer Cell Int. 2022;22(1):323. https://doi.org/10.1186/s12935-022-02743-3.
39. Fu S, Wang Y, Xia X, Zheng JC. Exosome engineering: current progress in cargo loading and targeted delivery. NanoImpact. 2020;20. https://doi.org/10.1016/j.impact.2020.100261.
40. Park O, Choi ES, Yu G, Kim JY, Kang YY, Jung H, et al. Efficient delivery of tyrosinase related Protein-2 (TRP2) peptides to lymph nodes using Serum-Derived exosomes. Macromol Biosci.

2018;18(12):e1800301. https://doi.org/10.1002/mabi.201800301.
41. Zou X, Yuan M, Zhang T, Wei H, Xu S, Jiang N, et al. Extracellular vesicles expressing a single-chain variable fragment of an HIV-1 specific antibody selectively target Env(+) tissues. Theranostics. 2019;9(19):5657–71. https://doi.org/10.7150/thno.33925.
42. Podolak I, Galanty A, Sobolewska D. Saponins as cytotoxic agents: a review. Phytochem Rev. 2010;9(3):425–74. https://doi.org/10.1007/s11101-010-9183-z.
43. Auquiere M, Muccioli GG, des Rieux A. Methods and challenges in purifying Drug-Loaded extracellular vesicles. J Extracell Vesicles. 2025;14(6):e70097. https://doi.org/10.1002/jev2.70097.
44. Lin M, Qi X-R. Purification Method of Drug-Loaded Liposome. VDI-Wärmeatlas. Springer Reference Technik2019. pp. 1–11.
45. Wang J, Chen D, Ho EA. Challenges in the development and establishment of exosome-based drug delivery systems. J Control Release. 2021;329:894–906. https://doi.org/10.1016/j.jconrel.2020.10.020.
46. Al-Jipouri A, Almurisi SH, Al-Japairai K, Bakar LM, Doolaanea AA. Liposomes or extracellular vesicles: A comprehensive comparison of both lipid bilayer vesicles for pulmonary drug delivery. Polym (Basel). 2023;15(2). https://doi.org/10.3390/polym15020318.
47. Levitan I. Evaluating membrane structure by Laurdan imaging: disruption of lipid packing by oxidized lipids. Curr Top Membr. 2021;88:235–56. https://doi.org/10.1016/bs.ctm.2021.10.003.
48. Harris MF, BBK, Bell DJ. Use of Laurdan fluorescence intensity and polarization to distinguish between changes in membrane fluidity and phospholipid order biochimica. Et Biophys. 2002;1565:123–8.
49. Di Scala C, Fantini J, Yahi N, Barrantes FJ, Chahinian H. Anandamide revisited: how cholesterol and ceramides control Receptor-dependent and receptor-Independent signal transmission pathways of a lipid neurotransmitter. Biomolecules. 2018;8(2). https://doi.org/10.3390/biom8020031.
50. Pfrieger FW, Vitale N. Cholesterol and the journey of extracellular vesicles. J Lipid Res. 2018;59(12):2255–61. https://doi.org/10.1194/jlr.R084210.
51. Skotland T, Sagini K, Sandvig K, Llorente A. An emerging focus on lipids in extracellular vesicles. Adv Drug Deliv Rev. 2020;159:308–21. https://doi.org/10.1016/j.addr.2020.03.002.